International Journal of Simulation, Optimization & Modelling
ISSN: 3083-967X

Investigation of Ship Motion and Liquid Sloshing Interaction under Wave Conditions

J. Muriban[1], G. S. Prayogo[2], J.M. Zikri[3], Rosidah M. Norsat[4], M. Isa Rahim[1]

[1]Centre for Research and Innovation, Jabatan Pendidikan Politeknik dan Kolej Komuniti, Malaysia
[2]Department of Mechanical Engineering, Politeknik Negeri Banyuwangi, Indonesia
[3]Faculty of Mechanical and Automotive Engineering Technology, Universiti Malaysia Pahang AlSultan Abdullah, Malaysia
[4]Centre for Automotive Engineering, Universiti Malaysia Pahang Al-Sultan Abdullah, Malaysia

Corresponding Author: jacklymuriban@gmail.com

Abstract
This paper investigates internal liquid sloshing within tanks and its impact on ship motion responses. The external ship response is determined using an impulse response function (IRF) method, while the internal flow within the tanks is modelled using the two-phase incompressible Reynolds-averaged Navier-Stokes (RANS) equations. A Volume of Fluid (VOF) technique is employed to capture violent flows, and the Finite Volume Method (FVM) is used for discretization. The viscous flow solver is developed within the open-source CFD framework, Open Field Operation and Manipulation (Open FOAM). A three-dimensional simplified LNG ship with two partially filled tanks in waves is analyzed. Numerical simulations are conducted to examine the coupled effects between ship motion and liquid sloshing, with validation performed accordingly. The results indicate that coupling effects are dominant under low filling conditions. The roll response amplitude operators (RAOs) exhibit a typical anti-rolling effect, where roll motion significantly decreases near ship motion resonance, and double peaks appear at sloshing motion resonant frequencies.

Article Info
Received: 20 March 2025
Revised: 27 April 2025
Accepted: 16 May 2025
Available online: 27 May 2025

Keywords
Ship Motion
Open FOAM
Impulse-Response Function
Coupling Effect
Sloshing
LNG-FPSO

1. Introduction

Maritime transportation plays a crucial role in global trade, with liquefied gas carriers, oil tankers, and container ships forming a significant portion of the global fleet (UN Conference on Trade and Development, 2023). These vessels frequently encounter dynamic environmental conditions, such as waves and wind, which induce ship motions that can influence stability, operational efficiency, and safety (Wang et al., 2024), Fig. 1 shows the sloshing phenomena at different tank fill heights and the actual internal view of the membrane LNG tank. Among the various factors affecting ship behaviour, liquid sloshing within partially filled tanks is a critical issue, particularly in vessels carrying liquefied natural gas (LNG) or liquefied petroleum gas (LPG) (Zhang et al., 2021, Hwang & Lee. 2021). The movement of liquid within tanks can generate significant hydrodynamic forces, which in turn affect the overall motion response of the ship, potentially leading to hazardous conditions such as excessive roll motion, reduced stability, and structural fatigue (Tang et al., 2021, Song et al. 2021).

To ensure the safe operation of ships, a comprehensive understanding of the coupled interactions between ship motion and internal liquid sloshing is essential. The phenomenon of liquid sloshing is governed by complex fluid dynamics, including nonlinear free surface deformations, wave breaking, and turbulence. In recent years, advancements in Computational Fluid Dynamics (CFD) have significantly improved the ability to predict these interactions with greater accuracy. Numerical simulations provide a cost-effective alternative to experimental testing, allowing researchers to study various filling conditions, wave environments, and tank configurations. However, despite these advancements, further research is required to enhance the accuracy of numerical models and to better understand the influence of liquid sloshing on ship stability under different sea conditions.

Several studies in recent years have focused on the numerical and experimental analysis of liquid sloshing and its effects on ship dynamics. Jiang et al. (2020) investigated the coupling effects of ship motion and liquid sloshing using a numerical approach based on the Reynolds averaged Navier-Stokes (RANS) equations, highlighting the significance of nonlinear sloshing behavior on roll motion. Wang and Kim (2021) employed the Volume of Fluid (VOF) method to study violent sloshing in LNG carriers, demonstrating the importance of free surface evolution in predicting sloshing-induced loads. Zhao et al. (2022) explored the anti-rolling effect of liquid sloshing tanks in wave environments, emphasizing the role of filling ratios in controlling roll amplitudes. Liu et al. (2023) developed a coupled CFD–multi-body dynamics model to examine ship motion responses in irregular seas, confirming that low filling conditions significantly amplify coupling effects. Additionally, (Kumar et al. 2008) presented a numerical approach for predicting the heave, pitch, and roll motions of a ship in waves using the RANSE method, which showed good agreement with experimental data. Further, investigated the effect of parametric rolling on ships using a numerical simulation method that accounted for nonlinear terms in the rolling equation (Chang, 2008). The role of numerical modelling in fluid dynamics and energy systems extends beyond ship hydrodynamics and has been widely applied in thermodynamic performance prediction (Muriban, 2023). Their studies on the principles of fluid-thermal interaction in confined systems provide valuable insights into the behaviour of internal liquid sloshing and its impact on surrounding structures. Moreover, Chen et al. (2024) recently introduced an improved numerical solver within the Open FOAM framework, achieving higher accuracy in predicting sloshing-induced forces. These studies demonstrate the ongoing progress in understanding ship-liquid interactions but also highlight the need for further research on optimizing numerical modelling techniques.

In this study, the internal liquid sloshing within partially filled tanks and its effects on ship motion responses are investigated through numerical simulations. The Impulse Response Function (IRF) method is applied to solve the external ship motion, while the two-phase incompressible RANS equations are used to model the internal flow. The Volume of Fluid (VOF) technique is employed to capture free surface dynamics, and the Finite Volume Method (FVM) is adopted for numerical discretization. Simulations are conducted on a threedimensional simplified LNG carrier with two partially filled tanks subjected to wave conditions. The objective of this study is to analyze the coupled interaction between ship motion and liquid sloshing, validate the numerical model, and provide insights into the impact of different filling conditions on roll motion response.

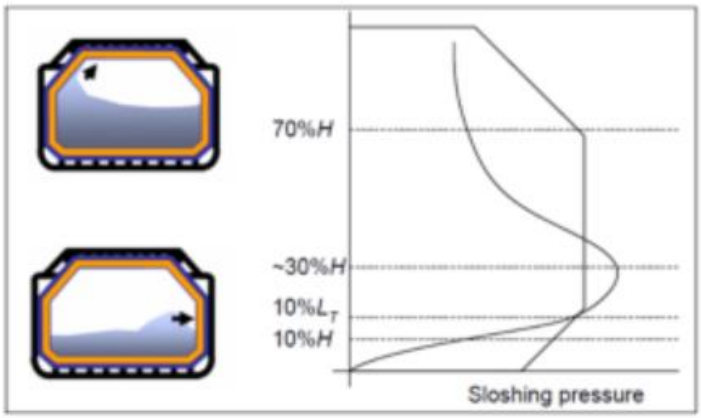

Fig. 1. Sloshing dynamics at different tank fill levels

2. Methodology

Mathematical formulation and numerical model (Internal sloshing flow model)

The internal fluid dynamics are modelled under the assumption of an incompressible flow. The governing equations for this motion are the Navier-Stokes equations, which are expressed as follows (Jiang et al., 2014):

$$\frac{\partial u_i}{\partial x_i} = 0 \tag{1}$$

$$\rho \frac{\partial u_i}{\partial x_t} + \rho \frac{\partial (u_j u_i)}{\partial x_j} - \rho \frac{\partial}{\partial x_j}\left(v \frac{\partial u_i}{\partial x_j}\right) = \rho \frac{\partial \rho}{\partial x_i} \tag{2}$$

where ui and uj denote velocity components, p represents pressure, ρ is fluid density, and v is the kinematic viscosity. Eq. (2) can be written in the vector form:

$$\frac{\partial \rho U}{\partial t} + \nabla (\rho U U) - \nabla (\mu \nabla U) = -\nabla \rho \tag{3}$$

To implement these equations within the Open FOAM computational framework, they are discretized using the FVM and solved using C++-based algorithms. The specific solver structure in Open FOAM is written as:

solve (f vm :: ddt (rho,U) + f vm :: div(phi,U) – fvm :: laplacian (mu,U) = - f vc :: grad (p))

where rho represents density, mu denotes viscosity, phi refers to volume flux, and fvm/fvc are Open FOAM classes for finite volume computations. The terms ddt(), div(), laplacian(), and grad() correspond to time derivatives, convective transport, diffusion, and pressure gradient terms, respectively. To accurately track free surface motion, the VOF method is applied. The governing equation for interface tracking is formulated as:

$$\frac{\partial \alpha}{\partial t} U \cdot \Delta \alpha = 0 \tag{4}$$

where α represents the volume fraction, with values of 0 indicating air and 1 representing water. The effective density and viscosity for the two-phase system are calculated as:

$$\rho = \varphi \rho_w + (1 - \varphi)\rho_a, \quad \mu = \varphi \mu_w + (1 - \varphi)\mu_a \tag{5}$$

where ρw, μw and ρa, μa are the density and viscosity of water and air, respectively. To ensure numerical stability, the Courant-Friedrichs-Lewy (CFL) condition is applied to determine the time step:

$$Cr = \frac{U \Delta t}{\Delta x} \leq 1/3 \tag{6}$$

where Cr is the Courant number, Δx represents the grid spacing, and U is the velocity magnitude. In this study, the Courant number is set to 0.1, and the time step is fixed at 0.001s to maintain numerical accuracy.

For numerical computations, the inter DyM Foam solver in Open FOAM is employed due to its capability of handling dynamic mesh adaptation. The selected numerical schemes include:

- Gauss cubic scheme for convective terms
- Gauss linear corrected scheme for Laplacian terms
- Gauss linear scheme for pressure gradients
- Euler implicit scheme for time integration

A turbulence model is also incorporated to approximate the Reynolds stress effects, while mesh refinement is applied near the wall boundaries and free surface region to improve resolution in critical areas.

Wave ship model and coupled strategy

The present study considers a scaled model of an LNG ship, as illustrated in **Fig. 2**, to analyze the coupled interaction between ship motion and internal liquid sloshing. The ship model and tank configurations follow a model-ship scale approach, ensuring that the numerical and experimental results remain consistent. The primary specifications of the tanks are detailed in **Table 1**, while the main particulars of the LNG ship are presented in **Table 2**. The numerical simulations incorporate hydrodynamic and sloshing parameters, including hull geometry, tank dimensions, wave excitation, and motion responses.

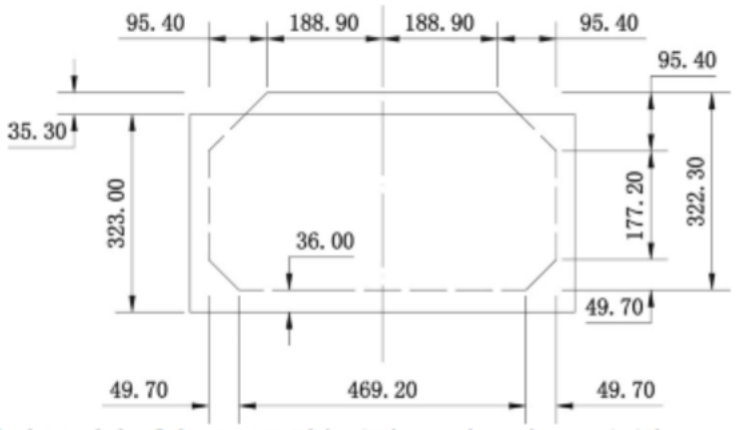

Fig. 2. Scaled Model of the LNG Ship (Dimensions in mm) (Jiang et al., 2015a)

A floating LNG vessel with partially filled tanks is considered. The ship motion is described using two reference coordinate systems:

a) A ship-fixed coordinate system, which moves with the vessel.
b) A space-fixed Cartesian coordinate system (X, Y, Z), centred at the vessel's centre of gravity.

The potential flow theory is applied to model external wave action on the hull. The incident wave profile is given by:

$$\phi = Ae^{i(kx-\omega t-\beta)} \tag{7}$$

where:
A = wave amplitude
ω = wave frequency
k = wave number
β = heading angle
ϕ = velocity potential

The Impulse IRF method is applied to determine the vessel's motion response. The ship motion equation is formulated as:

$$\sum_{j=1}^{6}\{[m_{ij} + a_{ij}(\infty)]\ddot{\xi}_j(t) + \int_0^t R_{ij}(t-\tau)\dot{\xi}_j(\tau)d\tau + c_{ij}\xi_{ij}(t)\} = F_i^{ext}(t) + F_i^{int}(t) \quad (8)$$

In this equation, mij represents the mass matrix, while a_{ij} (∞) denotes the added mass at infinite frequency. The retardation function, $R_{ij}(t)$, characterizes radiation damping effects over time. Additionally, c_{ij} corresponds to the hydrostatic restoring coefficient, which influences the vessel's stability. The external forces acting on the ship due to wave action are represented by Fi^{ext} (t), whereas Fi^{int} (t) accounts for the internal forces generated by liquid sloshing within the tanks.

The retardation function R_{ij}(t) is derived as:

$$R_{ij}(t) = \frac{2}{\pi}\int_0^{\infty} b_{ij}(\omega)\cos(\omega t)\,d\omega = -\frac{2}{\pi}\int_0^{\infty}\omega\{a_{ij}(\omega) - a_{ij}(\infty)\}\sin(\omega t)d\omega \quad (9)$$

where b_{ij} (ω) and a_{ij} (ω) represent damping coefficients and added mass, respectively. The added mass at infinite frequency is given by:

$$a_{ij}(\infty) = a_{ij}(\omega) + \frac{1}{\omega}\int_0^{\infty} R_{ij}(t)\sin(\omega t)dt \quad (10)$$

To account for roll damping, an equivalent linear damping coefficient is introduced:

$$v_{44}^{(1)} = 2\gamma\sqrt{\{m_{44} + a_{44}(\infty)\}c_{44}} \quad (11)$$

Table 1. Main particular of tanks (model-ship scale)

Parameters	Fore Peak (FP) tank (m)	After Peak (AP) tank (m)
l	0.4696	0.5660
b	0.4692	0.4692
h	0.3583	0.3583

Table 2. Main particulars of LNG Ship (model-ship scale)

Parameter	Dimension
Length between perpendiculars (L), m	2.85
Breadth molded on water line (B), m	0.63
Draught (T), m	0.13
Displacement volume molded (V), m 3	0.2200176
Radius of gyration, m ($KxxKyy$)	(0.1945, 0.7125)
Transverse GM, m	0.155
KG	0.165

Table 3. Filling conditions used in the present analysis

Case	Filling in FP tank	Filling in AP tank
A	25%	25%
B	60%	40%
C	85%	85%

Grid dependency tests

In the present numerical study, grid dependency analyses were performed to ensure the accuracy and stability of the computational model. Fine meshes were applied in the vicinity of the tank walls, while coarser grids were utilized in the remaining computational domain. To accurately capture viscous boundary layer effects, violent free surface oscillations, and impulsive pressures, the smallest square grids were placed near the waterline and tank wall corners. Grid dependency tests were conducted under (20%, 20%) filling conditions. Five different mesh resolutions were employed, considering an incident wave amplitude of A=0.500 m and a wave frequency of $\omega(L/g)^{1/2}$ =2.00 rad/s. The number of elements varied across the mesh configurations, with Mesh 1 consisting of 870 elements, Mesh 2 containing 1,800 elements, Mesh 3 having 25,840 elements, Mesh 4 comprising 92,800 elements, and Mesh 5 consisting of 219,960 elements. A typical mesh scheme for the AP tank at a 20% filling condition is illustrated in **Fig. 3**.

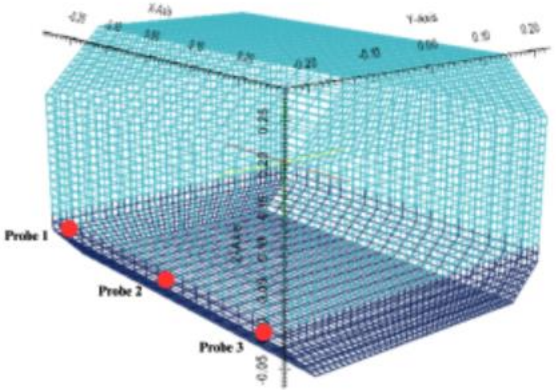

Fig. 3. A typical grid system in AP tank for 20% filling condition

To evaluate grid convergence, local sloshing pressure signals at a P2 probe location were analyzed for mesh configuration, as depicted in **Fig. 3**. The results obtained were found to be nearly identical for $\omega(L/g)^{1/2}$ =2.00 rad/s, indicating that further mesh refinement had minimal impact. Additionally, the results from Mesh 4 closely resembled those of the finer Mesh 5, while noticeable differences were observed when compared to the three coarser meshes, as shown in **Fig. 4**. It was therefore determined that Mesh 4 provided sufficient accuracy for obtaining convergent results, as the differences between Mesh 4 and Mesh 5 were significantly smaller than those observed among the other mesh configurations.

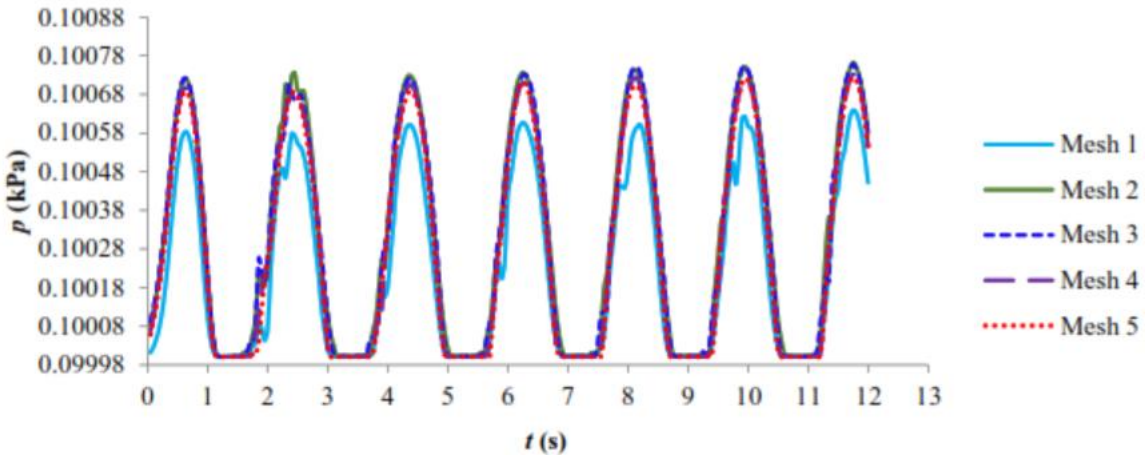

Fig. 4. Grid-dependency analysis of local pressure at probe P_2 for (20%, 20%) filling condition with A = 0.500 m, $\omega(L/g)^{1/2}$ = 2.00

Validation for coupling of internal sloshing and ship motions

A simplified LNG ship model with two partially filled tanks is used for numerical simulations. Towing-tank experiments using a 1/100 scale model have been previously conducted, and the corresponding

experimental data is referenced for validation (Jiang et al. 2015; Nam et al. 2009). The same experimental scale is adopted to ensure consistency between numerical and experimental analyses. Simulations are performed to assess the coupling effects between ship motion and internal sloshing, considering three degrees of freedom (DOF). Since these effects are more significant at low filling conditions, the heave and roll RAOs in head sea and beam sea are presented in **Fig. 5** and compared with previous experimental and numerical studies. The results show good agreement for heave RAOs in head sea and roll RAOs in beam sea, confirming the accuracy of the numerical model. However, some discrepancies appear in one referenced study, particularly for the specific filling conditions examined here.

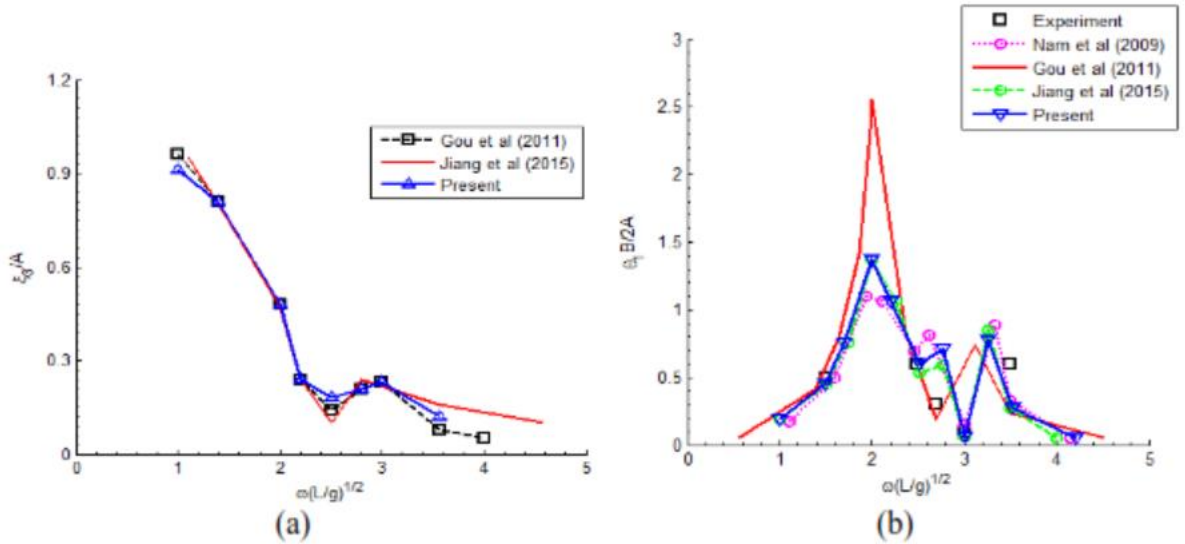

Fig. 5. (a) Heave RAOs of an LNG Ship at a (20%, 20%) filling condition in head sea; (b) Roll RAOs of an LNG with Wave Frequency at a (20%, 20%) filling condition in beam sea.

3. Result & Discussion

The roll motion of a ship in beam sea is strongly influenced by internal liquid sloshing, which can either amplify or dampen oscillations depending on the filling level. Fig. 6 presents the effect of liquid sloshing on ship roll RAOs under different filling conditions in beam sea, as detailed in Table 3. In all cases, the roll response reaches a peak near $\omega(L/g)^{1/2} = 2.5$ and then declines. In **Fig. 6(a)**, the (25%, 25%) filling condition shows a significant reduction in roll motion compared to the case without sloshing. However, noticeable fluctuations indicate that at lower filling levels, the sloshing motion is not fully synchronized with the ship's roll, leading to some irregularities. In **Fig. 6(b)**, the (60%, 40%) condition exhibits a more stable reduction in roll response, suggesting that an increased liquid volume enhances energy dissipation, thereby damping roll motion more effectively.

Meanwhile, **Fig. 6(c)** demonstrates that at (85%, 85%) filling, the damping effect is most pronounced, with a substantial reduction in peak roll amplitudes. This confirms that at higher filling levels, the liquid mass contributes significantly to stabilizing ship motion by counteracting roll oscillations. Overall, the results indicate that internal liquid sloshing plays a crucial role in modifying ship roll dynamics, with higher filling levels leading to more effective roll damping. However, at lower filling ratios, the interaction between the sloshing liquid and ship motion can introduce irregularities in roll response.

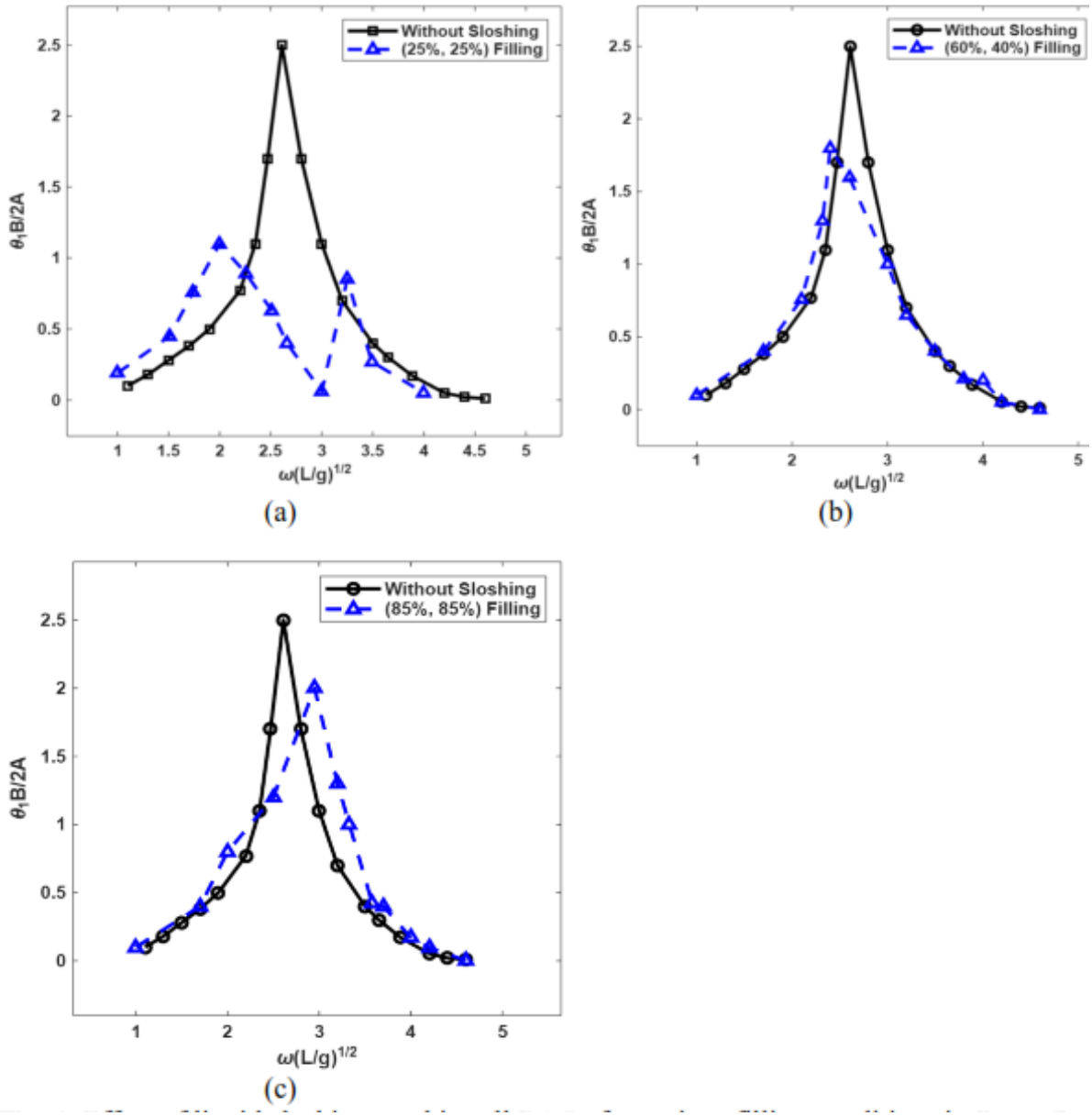

Fig. 6. Effect of liquid sloshing on ship roll RAOs for various filling conditions in Beam Sea: (a) (25%, 25%), (b) (60%, 40%), and (c) (85%, 85%)

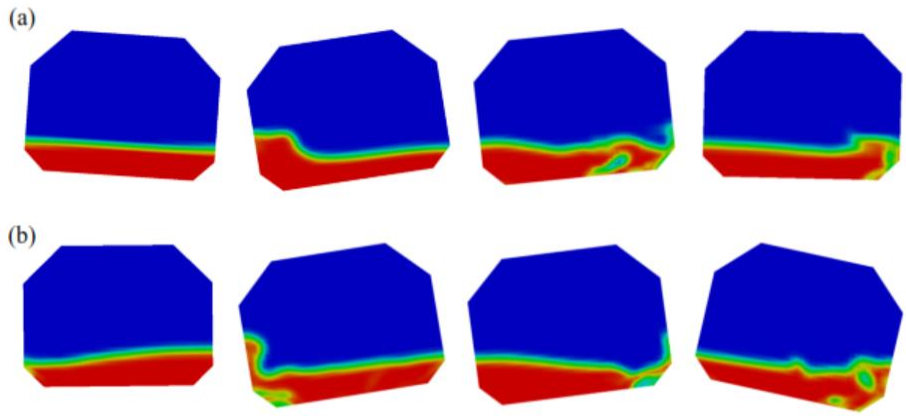

Fig. 7. Internal sloshing configurations at different incident wave amplitudes for (25%, 25%) filling condition: (a) $\omega(L/g)^{1/2} = 2.00$ and (b) $\omega(L/g)^{1/2} = 3.25$

Fig. 7 illustrates the internal sloshing flow configurations for a (25%, 25%) filling condition under different wave frequencies. At $\omega(L/g)^{1/2} = 2.00$ (**Fig. 7(a)**), the liquid remains relatively stable, with minor free surface deformations. However, at $\omega(L/g)^{1/2} = 3.25$ (**Fig. 7(b)**), more pronounced wave breaking and turbulence are observed, indicating stronger sloshing effects. The increased wave activity at higher frequencies leads to greater fluid motion, which can impact ship stability. These variations highlight the influence of wave frequency on internal liquid motion and the resulting dynamic loads on the tank structure.

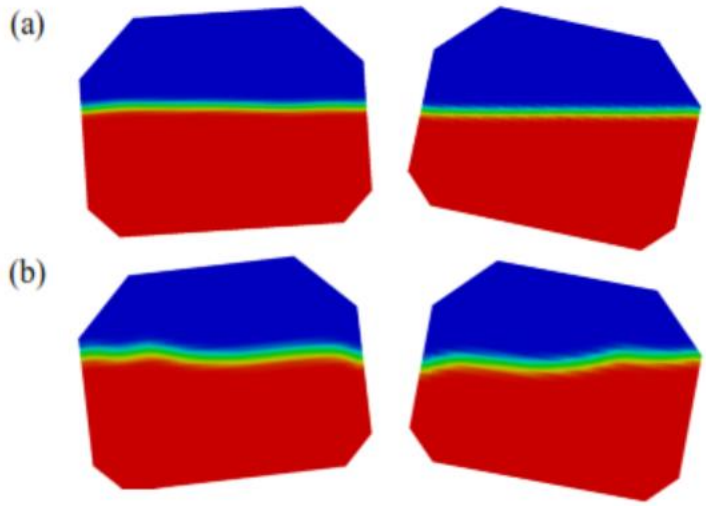

Fig. 8. Internal sloshing configurations at different incident wave amplitudes for (65%, 40%) filling condition: (a) $\omega(L/g)^{1/2} = 2.00$ and (b) $\omega(L/g)^{1/2} = 3.25$

Fig. 8 presents the internal sloshing configurations for a (65%, 40%) filling condition under different wave frequencies. At $\omega(L/g)^{1/2} = 2.00$ (**Fig. 8(a)**), the liquid surface remains relatively stable with minimal disturbances. However, at $\omega(L/g)^{1/2} = 3.25$ (**Fig. 8(b)**), noticeable free surface deformations appear, indicating increased sloshing activity. Compared to lower filling conditions, the higher liquid volume results in stronger surface tension effects, which moderate wave breaking. These results suggest that filling levels influence the intensity of internal sloshing, affecting the dynamic forces exerted on the tank structure.

4. Conclusion

This study investigated the coupled interaction between ship motion and internal liquid sloshing in partially filled tanks using numerical simulations. The results demonstrated that sloshing significantly influences ship responses, particularly in roll motion, where damping and anti-rolling effects were observed, especially at lower filling conditions. Additionally, the internal sloshing flow configurations revealed that increased wave frequencies lead to greater free surface deformations, with the sloshing impact varying based on filling levels. Overall, the findings confirm that liquid sloshing plays a crucial role in ship stability, particularly for LNG and LPG carriers. The numerical results were validated against previous studies, reinforcing the reliability of the approach. Future research should focus on improving numerical modelling techniques to enhance the accuracy of sloshing-induced force predictions and explore strategies to mitigate its impact on ship dynamics.

Acknowledgement

The authors would like to express their sincere gratitude to all individuals who contributed to the completion of this research. This work was fully supported through the collective efforts and

contributions of all authors. No external funding or financial support was received for the execution of this study.

References

Jiang, S. C., Teng, B., Bai, W., & Gou, Y. (2015a). Numerical simulation of coupling effect between ship motion and liquid sloshing under wave action. Ocean Engineering, 108, 140–154. https://doi.org/10.1016/j.oceaneng.2015.07.044

Chen, R., Gao, Y., & Zhang, M. (2024). Improved OpenFOAM solver for liquid sloshinginduced forces. Ocean Engineering, 283, 114789. https://doi.org/10.1016/j.oceaneng.2024.114789

Gou, Y., Kim, Y., & Kim, T. Y. (2011). A numerical study on coupling between ship motions and sloshing in frequency and time domain. In Proceedings of the 21st ISOPE Conference (pp. 158–164), Maui, Hawaii, USA.

Hwang, S.-Y., & Lee, J.-H. (2021). The numerical investigation of structural strength assessment of LNG CCS by sloshing impacts based on a multiphase fluid model. Applied Sciences, 11(16), 7414. https://doi.org/10.3390/app11167414

Jiang, S. C., Teng, B., Bai, W., & Gou, Y. (2015a). Numerical simulation of coupling effect between ship motion and liquid sloshing under wave action. Ocean Engineering, 108, 140–154. https://doi.org/10.1016/j.oceaneng.2015.07.044

Jiang, S. C., Teng, B., Bai, W., & Gou, Y. (2015b). Numerical simulation of coupling effect between ship motion and liquid sloshing under wave action. Ocean Engineering, 108, 140–154. https://doi.org/10.1016/j.oceaneng.2015.07.044

Jiang, S. C., Teng, B., Gou, Y., Lu, L., & Bai, W. (2014). Numerical simulation on coupled effect between ship motion and liquid sloshing under wave action.

Jiang, X., Li, Y., & Zhang, W. (2020). Coupled ship motion and liquid sloshing using RANS simulation. Ocean Engineering, 213, 107507. https://doi.org/10.1016/j.oceaneng.2020.107507

Kumar, R., Kim, Y., Kim, D. W., & Kim, Y. S. (2008). Numerical study on the heave, pitch, and roll motions of a ship in waves using the RANSE method.

Liu, B., Chen, X., & Wang, P. (2023). Coupled CFD–multi-body dynamics model for ship motion in irregular seas. Marine Structures, 88, 103486. https://doi.org/10.1016/j.marstruc.2023.103486

Muriban, J. (2023). Performance analysis of the rhombic drive beta-configuration Stirling engine. Journal of Social Sciences and Technical Education, 3(1), 1–10. http://myjms.mohe.gov.my/index.php/jossted

Nam, B. W., Kim, Y., Kim, D. W., & Kim, Y. S. (2009). Experimental and numerical studies on ship motion responses coupled with sloshing in waves. Journal of Ship Research, 53(2), 68–82. https://doi.org/10.5957/JSR.2009.53.2.68

Sheng-Chao, J., et al. (2015). Numerical simulation of coupling effect between ship motion and liquid sloshing under wave action. Ocean Engineering, 108, 140–154.

Song, L., Deng, J., Lu, J., Wang, B., & Xue, D. (2021). Transient response analysis of multilayer sloshing fluid in LNG tank. Journal of Physics: Conference Series, 2076(1), 012024. https://doi.org/10.1088/1742-6596/2076/1/012024

Tang, Y., Liu, Y., Chen, C., Chen, Z., He, Y., & Zheng, M. (2021). Numerical study of liquid sloshing in 3D LNG tanks with unequal baffle height allocation schemes. Ocean Engineering, 234, 109181. https://doi.org/10.1016/j.oceaneng.2021.109181

UN Conference on Trade and Development. (2023). Review of maritime transport 2023: Towards a green and just transition. UN-iLibrary. https://doi.org/10.18356/9789213584569

Wang, H., & Kim, Y. (2021). Numerical investigation of violent liquid sloshing in LNG carriers using the volume of fluid method. Applied Ocean Research, 111, 102579. https://doi.org/10.1016/j.apor.2021.102579

Wang, Y., Jiang, S., & Zhou, T. (2024). Experimental and numerical investigation on ship rolling motion response coupled with liquid sloshing. https://doi.org/10.1115/OMAE2024-125601

Zhang, Q., Zhu, H., & Wei, W. (2021). Numerical simulation on the sloshing characteristics of gas-liquid flow in cargo tanks and anti-sloshing methods. Journal of Physics: Conference Series,

1746(1), 012046. https://doi.org/10.1088/1742-6596/1746/1/012046
Zhao, T., Sun, H., & Liu, J. (2022). Anti-rolling effects of sloshing in partially filled tanks. Journal of Sound and Vibration, 527, 117153. https://doi.org/10.1016/j.jsv.2022.117153